**ISSN: 2584-0495** **Vol. 2, Issue 12, pp. 1447-1454**

IJMIT International Journal of Microsystems and IoT

International Journal of Microsystems and IoT

**ISSN: (Online) Journal homepage: https://www.ijmit.org**

# Transport, EMISE and Humidity Sensing studies of Polyaniline-Cobalt Ferrite Nanocomposites

**Raghavendra Naik, M. Revanasiddappa, Manjunatha. S and Y.T. Ravikiran**

**Cite as:** Raghavendra, N., M., R., Manjunatha., S., & Y.T., R. (2024). Transport, EMISE and Humidity Sensing studies of Polyaniline-Cobalt Ferrite Nanocomposites. International Journal of Microsystems and IoT, 2(12), 1447–1454. https://doi.org/10.5281/zenodo.15455767

DOI: https://doi.org/10.5281/zenodo.15455767

International Journal of Microsystems and IoT
Vol.2, Issue 12, pp.1440-1446; DOI:
https://doi.org/10.5281/zenodo.15455767

# Transport, EMISE and Humidity Sensing studies of Polyaniline-Cobalt Ferrite Nanocomposites

Raghavendra Naik[1], M. Revanasiddappa[1*], Manjunatha. S[2] and Y.T. Ravikiran[3]

[1] Department of Chemistry, PES University, Electronic city campus, Bangalore, India, 560100.
[2] Department of Physics, Kishida University, Ballari, 583104, India.
[3] Department of Physics, First Grade Government College, Holalkere, 577526, India.

**ABSTRACT**
Polyaniline-$CoFe_2O_4$ nanocomposite thin films and pellets were prepared by incorporating varying amounts of $CoFe_2O_4$ in the matrix of polyaniline (PANI) through an in-situ polymerization technique. Morphology of the composites were examined using SEM, XRD studies exhibited crystalline nature of the composites and FTIR analysis revealed cobalt ferrite was homogeneously mixed in the matrix of PANI. AC Conductivity, dielectric and electric modulus studies exhibited the regular behavior of PANI composites were studied in the range 10 Hz – 7 MHz Thin films of PANI- $CoFe_2O_4$ nanocomposites when exposed to a broad Frequency range: 2–3 GHz. showed electromagnetic interference in the range of -4 dB to -9 dB, indicating effective attenuation of electromagnetic energy and serving as evidence for EMI shielding. PANI has a more efficient conducting mechanism in CoFe2O4-PANI composites, according to conductivity experiments. The humidity sensitivity experiment revealed a variation in resistance in response to relative humidity when the pellets were exposed to a broad humidity range from 11% to 97% RH.

**KEYWORDS**
Nano composites
Agglomerate
Accumulate
Dissipation
PANI/$CoFe_2O_4$

## 1. INTRODUCTION

These days, PANI becoming more popular because of its special qualities, which include low weight, flexibility, ease of use, and inexpensive production. They are utilized in products like energy storage devices and super capacitors due to their special qualities, such as conductivity [1], [2]. Polymers that are generated by oxidative polymerization processes can have their conductivity increased and utilized in advanced technologies of the future by mixing them with metal oxide nanoparticles [3], [4].

Reconstituted aniline monomer is the building block of PANI, which is composed of alternate arrangements of a single (σ) and double (π) bond. The polymer's charge carriers polarons and solitons, are insufficient on their own to give the polymer conductivity [5], [6], [7]. $CoFe_2O_4$ nanoparticles that have been blended increase conductivity by producing holes and electrons, which act as charge carriers. Holes made by electrons travelling to nearby holes and jumping of electron forms new holes [8], [9]. $CoFe_2O_4$ nanoparticles are a form of semiconductor with both conducting and magnetic characteristics [10]. These nanocomposites improve the electromagnetic interaction by absorbing and reflecting radiation. It is beneficial in preventing increased radiation pollution and lowering undesired radiation in electronic and communication devices [11]. PANI is porous nature so allowing water molecules to enter it. This feature makes it suitable for use in humidity sensors in agriculture and the food industry[12].

Our work focused on producing several composites of PANI/$CoFe_2O_4$ nano composite, which were then evaluated using XRD, Fourier transform IR, and scanning electronic microscopy techniques.

## 2. EXPERIMENTAL

### 2.1 Materials and Methods

Every chemical utilized in this investigation was research-grade purity. Ammonium persulfate (APS), hydrochloric acid (HCl), aniline (C6H5NH2), and cobalt ferrite (CoFe2O4). Aniline was double-distilled to produce the nanocomposite, and deionized water was utilized to purify the polymer nanocomposites.

### 2.2 Preparation polyaniline

The oxidizing agent used in the oxidative polymerization process to produce polyaniline was ammonium persulfate (APS). Ammonium persulfate solution was added dropwise to the aniline and hydrochloric acid solution at a lower temperature after aniline had been dissolved in HCl solution. The entire liquid was continuously stirred for four to five hours using a magnetic stirrer in order to create powder of dark green color polyaniline. Polyaniline was purified by repeatedly washing it in ethanol and deionized water.

### 2.3 Preparation of polymer cobalt ferrite nanocomposites

By using the in-situ polymerization process, varying amounts of 2, 4, 6, 8, and 10% $CoFe_2O_4$ nanocomposite with aniline were added to create PANI/ $CoFe_2O_4$nanocompostes.

First, 40 ml of HCl solution and 1 ml of aniline are combined with a known proportion of cobalt ferrite, and the mixture is kept in an ice bath at a temperature below 5 °C. A 40 ml HCl solution mixed with APS in different beaker and resulting solution is then introduced drop wise in to first solution. after 4–5-hour continuous stirring precipitate was obtained. After washing the resulting precipitate with ethanol and double-distilled water, it is dried at 70°C for ten hours.

## 3. CHARACTERIZATION

FT-IR spectroscopic data was obtained using Nicolet 750 FTIR instrument in the frequency range 250 - 4000 cm$^{-1}$. The composite's surface morphology was investigated using a [Zeiss Ultra 60] scanning electron microscope (SEM). XRD data was obtained by using Malvern panalytical aeris bench top model.

### 3.1 Ac conductivity measurement

An hour was spent grinding a synthetic PANI/CoFe2O4 nanocomposite with a mortar and pestle. A thin pellet was created by applying five tons of hydraulic pressure to the nanocomposite. In the frequency range of 10 Hz to 7 MHz, the AC response characteristics of the nanocomposite pellet were recorded using a digital LCR meter [make: Hioki model 3532-50].

### 3.2 Humidity sensing measurement

The silver paint-coated pellets were used for humidity sensing studies. A digital Multimeter (HIOKI DT4282) was used to measure the resistance of these pellets under relative humidity environments at room temperature.

### 3.3 EMI shielding measurement

PANI/$CoFe_2O_4$ nanocomposites EMI shielding was investigated using the S band frequency range 2–3 GHz. The wave guide was filled with films of PANI/$CoFe_2O_4$ nanocomposites. The Tektronix spectrum analyzer receives the output from the signal generator (RIGOL), which is coupled to the input of a rectangular wave guide. The analyzer captures the residual frequency. Additionally, a computer-interfaced data recorder has been used to record frequency[13].

## 4. RESULT AND DISCUSSION

### 4.1 TIR analysis

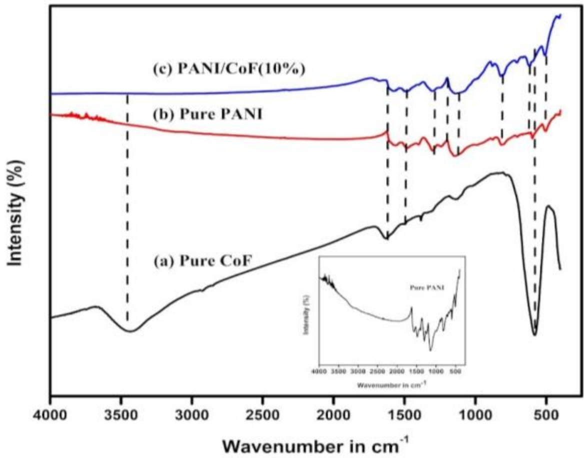

**Fig. 1** spectra of (a)Pure $CoFe_2O_4$, (b) Pure PANI, (C)10% PANI/$CoFe_2O_4$.

The FT-IR spectra of pure polyaniline, pure $CoFe_2O_4$ and its 10% composite of PANI/$CoFe_2O_4$ composite are displayed in Fig.1. It displays stretch at 590 cm$^{-1}$, which is the frequency at which the $CoFe_2O_4$ spinal structure stretches as a result of Fe-o vibration, whereas C-H bending out of the plane in the substitute benzene ring is seen at 780cm$^{-1}$. The large peak at 1150 cm$^{-1}$ indicates the presence of the N=Q=N (Q=quinoic) ring in vibration mode. The -C=N imine group found in polyaniline is represented by the vibration seen in 1507cm$^{-1}$. It displays an N-H stretching vibration caused by protonation in the 3500 cm$^{-1}$ regions. The strong peak at 570 cm$^{-1}$ found in pure PANI is absent in $CoFe_2O_4$ nanocomposites due to disturbance in the random configurations of PANI chains caused by CoFe2O4 and the PANI matrix, resulting in a more amorphous area and undetectable vibrations. This further extends or dilutes the intensity of FT-IR peaks.[14], [15].

### 4.2 XRD STUDIES

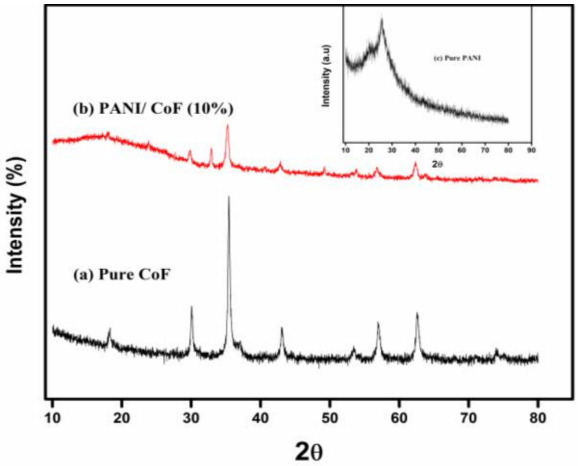

**Fig. 2** XRD images of (a) Pure $CoFe_2O_4$, (b) 10% PANI/$CoFe_2O_4$, (c) Pure PANI.

X-RD analysis confirms nature of pure PANI with pure cobalt ferrite and 10% PANI/$CoFe_2O_4$ composite. The pattern of pure cobalt ferrite and polyaniline composite is depicted in Fig .2. The XRD pattern of PANI shows large diffraction peaks at 2θ-19° and 20°, which suggest that it is semicrystalline. A sharp peak may be seen at 2θ - 19°, 30°, 36°, 43°, 54°, 57°, and 63° in the $CoFe_2O_4$ XRD pattern. The cobalt ferrite's crystallinity is confirmed by these pointed peaks. PANI composite the X-RD pattern of PANI/$CoFe_2O_4$ nanocomposites displays peaks at 2θ - 30°, 32°, 36°, 43°, 54°, 57°, and 63°. This shows that pure $CoFe_2O_4$ distributed in polyaniline shows interaction and create an ionic link with the polyaniline's amide group[16] [17], [18].

### 4.3 SEM ANALYSIS

PANI, cobalt ferrite and their composite has been investigated using a scanning electron microscope (SEM). It shows surface features, shown in Fig.3. (a) That a globular agglomeration was formed and interconnecting polymer chain bonds caused a chemically heterogeneous morphology to be dispersed unevenly. In Fig.3 (b) Pure $CoFe_2O_4$ typical structure of cobalt ferrite is granular, non-uniform, spherical with low crystallinity that appears uneven and porous. Fig.3 (c) Composites demonstrate how dispersant metal oxide microstructure agglomerated clusters form in the PANI matrix. [19] [20], [21].

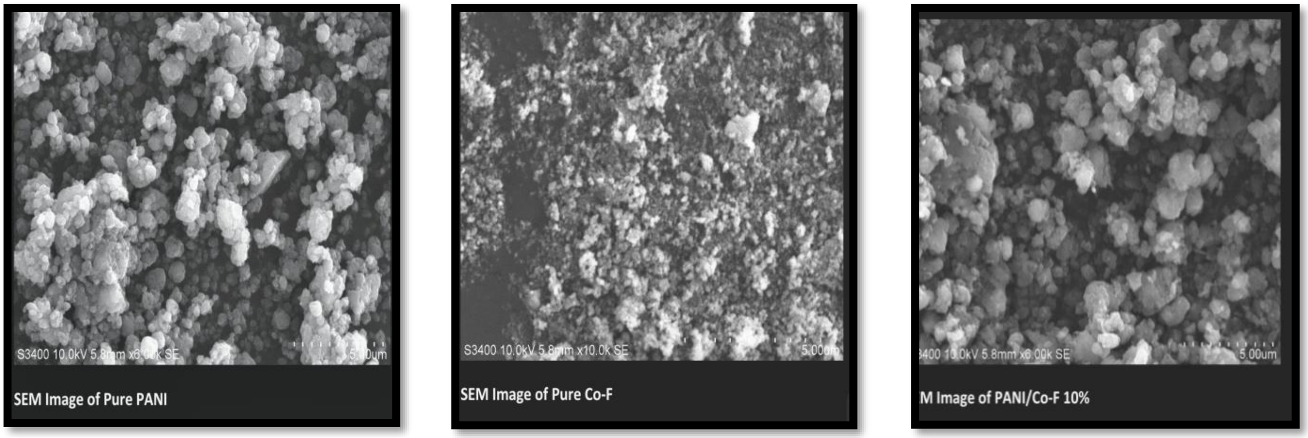

**Fig. 3** SEM pictures of (a) Pure PANI, (b) Pure $CoFe_2O_4$, (C)10% PANI/$CoFe_2O_4$

## 5. AC CONDUCTIVITY

Different PANI/ $CoFe_2O_4$ composites were subjected to 50 Hz to 1 MHz in order to perform the AC conductivity experiment. Conductivity values are measured by using the formula Equation $\sigma (f) = \sigma' (f) - \sigma'' (f)$ (1)
The real and imaginary components of AC conductivity are denoted by σ″ (f) and σ′ (f). The measurement of AC conductivity is shown in Fig.4. (a) and (b).

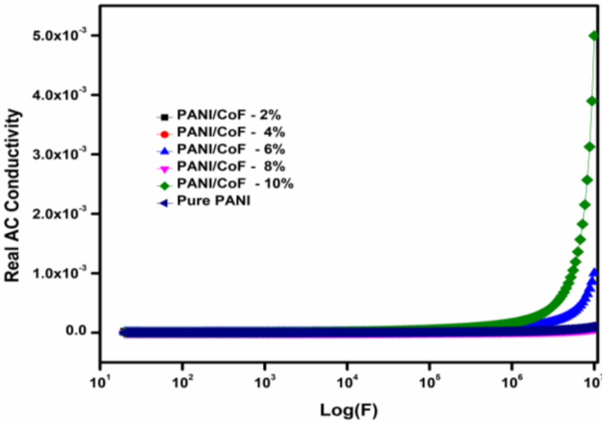

**Fig. 4(a)** Measurement of real AC conductivity for PANI/CoFe2$O_4$ at frequencies of 2, 4, 6, 8, and 10%.

Fig .4 (a) The composition demonstrates how the frequency of the different composite changes as the applied electric field increases. 10% and 6% composites exhibit the highest ac conductivity as compared to other composites; their frequency increases linearly. It indicates that charge carriers take longer at the interface at low frequencies, whereas polarization rises at high frequencies due to the charge's inability to keep up with the rapid changes in the electric field. A material will therefore display different electric characteristics based on the frequency of the applied field [22].

An imaginary portion of AC conductivity is depicted in Fig .4 (b) There is diversity in the AC conductivity of different composites when an external electric field is introduced. All composites initially exhibit the same AC conductivity at low frequencies; at higher frequencies, conductivity increases by 10% and 6%, respectively. Accept these two composites at higher frequencies; other composites don't change at high frequencies.

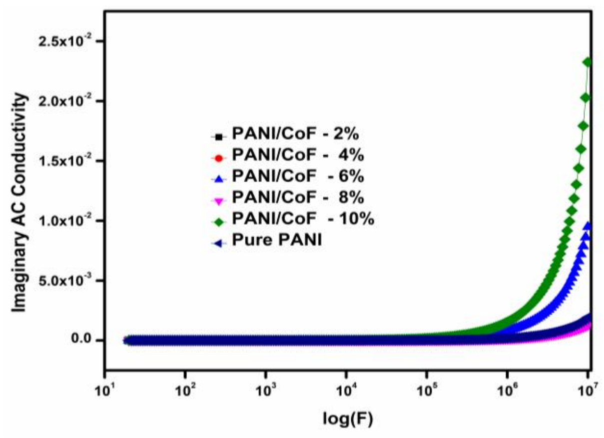

**Fig. 4(b)** Measurement of imaginary AC conductivity for PANI/CoFe2O$_4$ at frequencies of 2, 4, 6, 8, and 10%.

### 5.1 Dielectric studies

The dielectric constant measures a material's ability to polarize when an electric field is applied. The manner in which a material transmits and stores external electric energy determines this. The dielectric constant is plotted against the applied electric field in the Fig.5 (a) The dielectric constant drastically drops with increasing frequency because of space charge polarization, which is seen at lower frequencies for composite concentrations of 2%, 6%, and 10%. $CoFe_2O_4$ nanocomposites exhibit various electrical characteristics in PANI. A high-frequency electric field exhibits a rapid change in the electric field and reduces charge accumulation at the interface, while larger concentrations cause charge carriers to concentrate at the interface, increasing the dielectric constant. There was less polarization[23], [24].

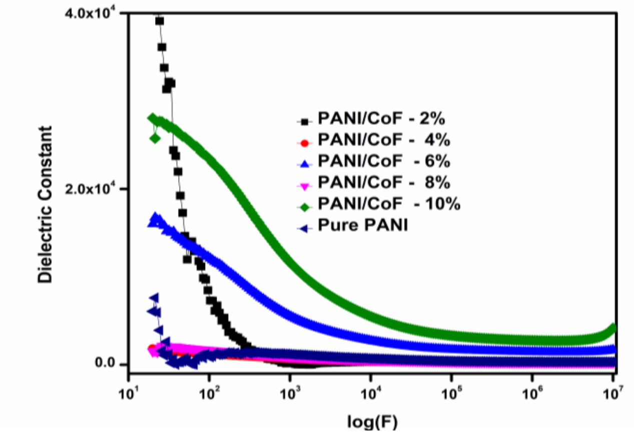

**Fig. 5 (a)** The real dielectric constant for PANI/$CoFe_2O_4$ varies by 2, 4, 6, 8, and 10% depending on the frequency applied.

It shows the imaginary dielectric constant in Fig.5. (b) It depicts the energy loss as heat brought on by the trailing dipole's dielectric loss. 2%, 4%, 6%, 8%, and 10% polymer composites were subjected to the frequency.

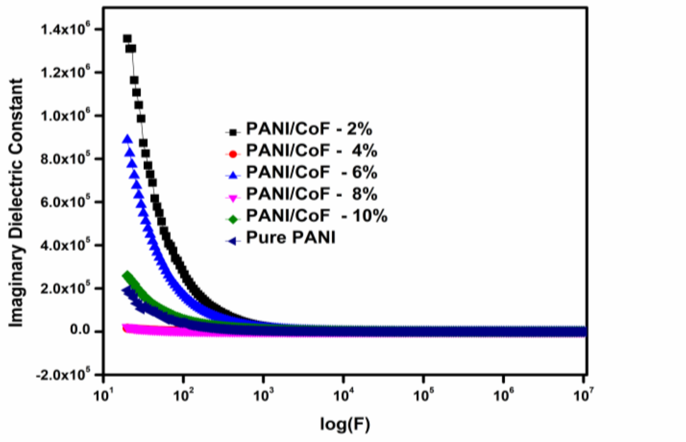

**Fig. 5 (b)** The imaginary dielectric constant for PANI/$CoFe_2O_4$ varies by 2, 4, 6, 8, and 10% depending on the frequency applied.

Lower frequencies have a lesser imaginary dielectric constant; as the frequency rises, it falls. This demonstrates that it takes time for the dipole to align itself with an applied external electric field. The dipole is currently in charge of energy release and dissipation in the form of heat, phase lag raises the amount of energy wasted as heat, which causes dielectric loss and lowers the material's storage capacity efficiency[22].
The dielectric modulus with frequency is displayed in Fig .6. which analyzes the permittivity.

Eq .1 $M* = M' + M''$ (2)

Here, M' and M" represent the dielectric modulus' real and imaginary components, respectively. The composite exhibits frequency variation in Fig.6 (a) 6% and 10% of nanocomposites do not exhibit change when the applied electric frequency increases, indicating greater polarization. This is because modulus and material polarization are inversely correlated, indicating that the material can store more energy in an applied electric field. In other composites, short-range charge carriers are demonstrated by the dielectric modulus increasing with frequency[24].

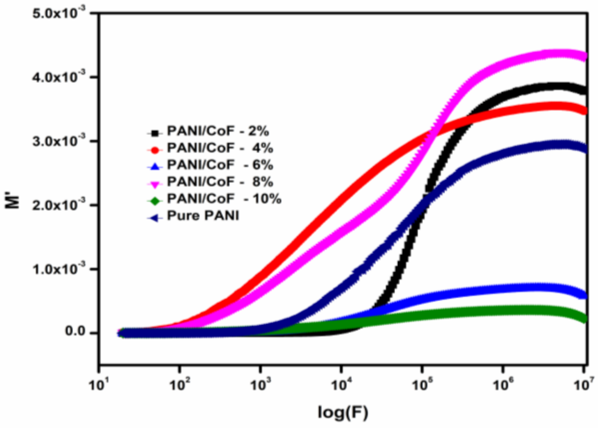

**Fig. 6 (a)** Displays the PANI/$CoFe_2O_4$ composites real dielectric modulus (M+) as a function of applied frequency for 2, 4, 6, 8, and 10%.

The imaginary dielectric modulus is displayed in Fig.6. (b) It depicts interfacial polarization-induced relaxation is represented by the imaginary electric modulus.

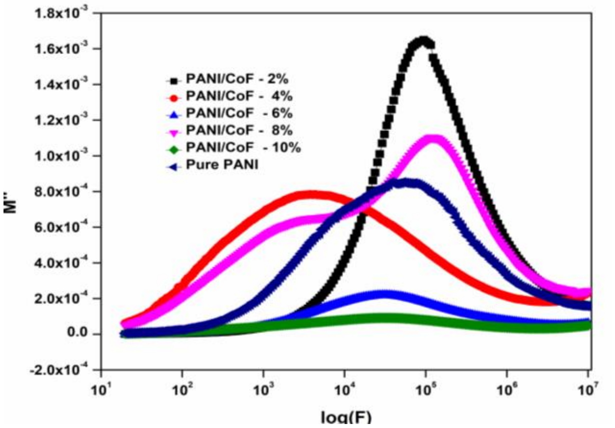

**Fig. 6 (b)** Displays the PANI/$CoFe_2O_4$ composites imaginary dielectric modulus (M") as a function of applied frequency for 2, 4, 6, 8, and 10%.

As the frequency increases, the electric modulus of 10% composites decreases. Variation appears in other composites more frequently. Because the 10% composite contains more nanocomposites, is larger in surface area, exhibits greater contact, and has fewer charge carriers, more charge builds up at the interface, increasing polarization.

## 6. EMI SE MEASUREMENT

**Table. 1** Cross platform comparative performance

| Shielding material | Shielding performance (dB) | Thickness (mm) | Frequency Region (GHz) | Reference |
|---|---|---|---|---|
| $CoFe_2O_4$/PANI | - 9 | 0.20 | 2-3 | Present work |
| $CoFe_2O_4$/PANI | - 4 | 0.25 | 2-3 | Present work |
| $CoFe_2O_4$/PANI | -50 | 5.0 | 9-12 | [25] |
| $CoFe_2O_4$/PANI | -40 | 5.0 | 9-12 | [25] |

Electromagnetic interference is becoming more prevalent as people rely more and more on contemporary wireless technological devices. Unwanted electromagnetic radiation from external sources is referred to as EMI interference [26].It can create a variety of issues, including increased current flow in circuits, voltage fluctuations, and noise in electronic devices [2], [27]. EMI shielding is essential to the effectiveness of the gadgets we use, including phones, laptops, TVs, and medical and military equipment[28]. Materials with the ability to prevent interference Using waveguide transmission line technology, the efficacy of EMI shielding for PANI/$CoFeO_4$ nanocomposite films has been evaluated here.

The results are used to Illustrate a frequency (GHz) vs. EMI shielding (dB) graph, and it is found that the EMI shielding of various polymer nanocomposites is nearly identical. The composites exhibit a -4 dB to -9 dB range of EMI shielding. All these composites show the same trend in shielding the EMI in S band.

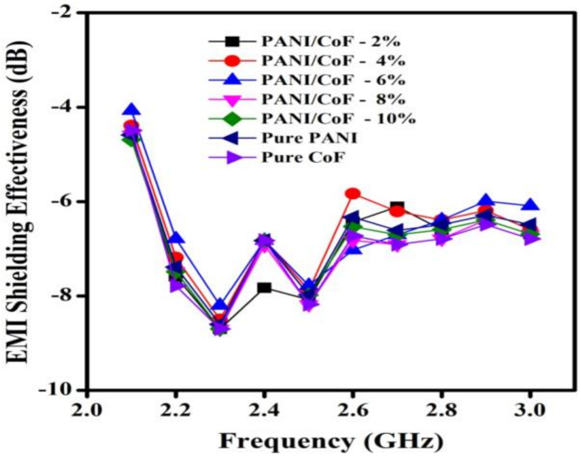

**Fig. 7** Frequency vs. EMI SE of PANI/$CoFe_2O_4$ composites of 2,4,6,8 an 10%

It's evident from the Fig.7. fluctuations that conductivity and EMI shielding efficacy are correlated. PANI is a conjugated conductive polymer that initially exhibits conductivity because of the π electrons' delocalization. Different concentrations of cobalt ferrite ($CoFe_2O_4$) nanocomposites are added to the polyaniline, creating an interconnecting network that increases the number of holes and electrons and facilitates easy electron mobility within the network of the polyaniline nanocomposite [29]. Conductivity is raised by this. Higher conductivity composites protect from electromagnetic radiation by absorbing more of it and producing a heating effect [30]. Reduced reflection results from a rise in EMI radiation absorption level with an increase in nanocomposite quantity. Because of the highest absorption at -9 dB, it appears that interfering electromagnetic radiation can be blocked in this range [31], [32].

$FSPL= 20 \log 10(d) + 20 \log 10(f) + 20 \log 10(4\pi/C) - GTX - GRX \quad (3)$

The aforementioned formula, which takes into account factors like film thickness (t), electrical conductivity and (σ) frequency (f) in MHz, can also use to calculate the effectiveness of EMI shielding.

## 7. HUMIDITY SENSING MEASUREMENT

PANI exhibits both the reduced form (-NH-) and the oxidized form (-N=) during synthesis because ammonium persulfate (APS), an oxidizing agent, is used in the process. $N \rightarrow NH^+$ and $N \rightarrow NH_2^+$ are the reduced and oxidized forms of nitrogen, respectively, due to the one unbonded electron pair on nitrogen[33]. It exhibits an electron hopping process as it transitions from the protonated reduced form (NH2+) to the protonated oxidized form (NH+). It is not until the proton is removed from ($NH_2^+$) that the electrons are lost. The proton transfer process is hampered when there is an increase in water adsorption in the polymer nanocomposite. As a result, resistance rises in tandem with humidity absorption.

As may be seen clearly from looking at the Fig. 8. (a) and (b) that resistance rises in tandem with humidity levels. SEM has already demonstrated the porous nature of the use PANI composite. As water molecules come into contact with the PANI/$CoFeO_4$ surface, they are physically adsorbed and a chemisorption mechanism is subsequently displayed [34]. $H^+$ and $OH^-$ hydroxide ions are first formed when water molecules collide on the surface[35], [36]. At this point, the polymer nanocomposites surface double hydrogen bond is adsorbed with the water molecules. The adsorption process begins when the $OH^{+3}$ ion attracts the $OH^-$.

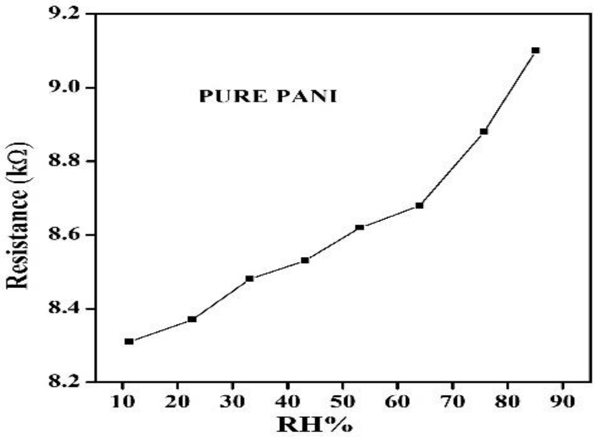

**Fig. 8 (a)** Resistance of pure PANI/ $CoFe_2O_4$ composites varies with percentage relative humidity.

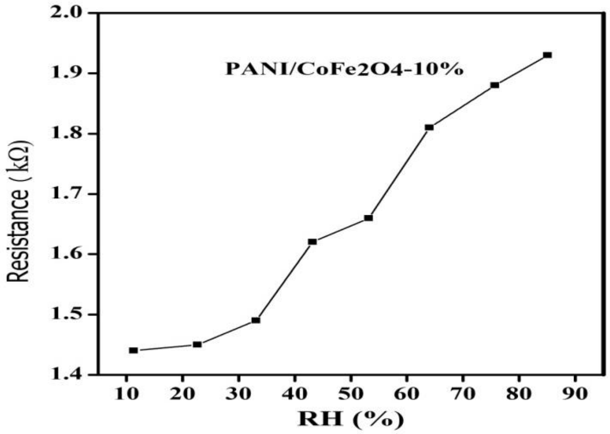

**Fig. 8 (b)** Resistance of 10% PANI/ $CoFe_2O_4$ composites varies with percentage relative humidity.

Water molecules combine with $OH^-$ ions to generate $HO^{+3}$ ions as physisorption rises. These ions then begin to migrate between two water molecules, further boosting absorption.

$H+ + OH \rightarrow H_2O$

$H_2O + H^+ \rightarrow H_3O^+$

More water vapor starts to accumulate between the polymer nanocomposites layers as a result of this process. It is the Grotthuss mechanism this explains hopping mechanism[37].

The humidity response of 10% PANI/ $CoFe_2O_4$ varies with polyaniline, as shown in Fig .8 (a) and (b). Cobalt ferrite, which has superior conductivity to pure polyaniline, is the primary factor causing the resistance change in PANI/CoFe2O4 nanocomposites. Polymer chains and silver particles separate due to the adsorption of water molecules when exposed to a humid environment, which results in low electrical conductivity. This indicates that the chemical makeup of the polymer and its composites affects humidity sensing[38].

## 8. CONCLUSION

PANI/$CoFe_2O_4$ nanocomposites were successfully made by in-situ polymerization method. The prepared composites have been characterized by using SEM, X-RD and FT-IR were performed to access the structural characteristics of the nanocomposites. Semi-crystalline structure of conducting polymer and $CoFe_2O_4$ is revealed by XRD. The FT-IR confirms characteristic bands of polyaniline and cobalt ferrite, the polyaniline at 1507 $cm^{-1}$ was due to presence of C=N and $CoFe_2O_4$ characteristic frequency band at 590 $cm^{-1}$ because of M-O bond. The SEM image reveals the agglomeration of polyaniline matrix and PANI/$CoFe_2O_4$ composites showed microstructure agglomerated clusters were seen. This polymer composite's conducting ability was investigated under applied frequency, and the results indicate that conductivity rose as the composite's PANI/$CoFe_2O_4$ (10%) content increased at this concentration the conducting path was created in the conducting polymer matrix. Composites materials tested in the frequency range of 2-3 GHz for EMI shielding effectiveness absorption values were -4 dB to -9 dB value effective. This means they have good AC electrical conductivity and are useful for EMI shielding of electronic devices. This indicates their suitability for EMI shielding in electronic devices. The increase in concentration of $CoFe_2O_4$ with composition up to about 10% improves moisture sensitivity hence its applicability in manufacture of sensor devices responsive to humidity.

## 9. ACKNOWLEDGEMENT

The authors would like to express their gratitude to the management of PES University, Electronic City Campus, Bangalore, and the Vision Group on Science and Technology for their support in carrying out this research work, under the grant PESUIRF/Chemistry-
ECC/2020/14 dated 30-09-2020.

## REFERENCES

1. "Critical review on recent developments in conducting polymer nanocomposites for supercapacitors - ScienceDirect." Accessed: Oct. 24, 2024. https://www.sciencedirect.com/science/article/abs/pii/S0379677923000486
2. L. T. Zegebreal, N. A. Tegegne, and F. G. Hone, "Recent progress in hybrid conducting polymers and metal oxide nanocomposite for room-temperature gas sensor applications: A review," *Sens. Actuators Phys.*, vol. 359, p. 114472, Sep. 2023, doi: 10.1016/j.sna.2023.114472.
3. "Conducting polymers prepared by oxidative polymerization: polyaniline - ScienceDirect." Accessed:Oct.25,2024. https://www.sciencedirect.com/science/article/abs/pii/S0079670098000082
4. "Conductive Polymer-Assisted Metal Oxide Hybrid Semiconductors for High-Performance Thin-Film Transistors | ACS Applied Materials & Interfaces." Accessed: Oct.25,2024. https://pubs.acs.org/doi/10.1021/acsami.0c21134
5. "Role of conducting polymer and metal oxide-based hybrids for applications in ampere metric sensors and biosensors - ScienceDirect." Accessed: Oct.25,2024. https://www.sciencedirect.com/science/article/abs/pii/S0026265X18318587?via%3Dihub
6. "Rev. Mod. Phys. 60, 781 (1988) - Solitons in conducting polymers." Accessed: Oct. 25, 2024. https://journals.aps.org/rmp/abstract/10.1103/RevModPhys.60.781
7. "Polarons, bipolarons, and solitons in conducting polymers | Accounts of Chemical Research." Accessed:Oct.25,2024. https://pubs.acs.org/doi/abs/10.1021/ar00118a005
8. N. K and C. Sekhar Rout, "Conducting polymers: a comprehensive review on recent advances in synthesis, properties and applications," *RSC Adv.*, vol. 11, no. 10, pp. 5659–5697, 2021, doi: 10.1039/D0RA07800J.
9. "Review on Optical and Electrical Properties of Conducting Polymers - Bajpai - 2016 - Indian Journal of Materials Science - Wiley Online Library." Accessed: Oct. 25, 2024. https://onlinelibrary.wiley.com/doi/10.1155/2016/5842763
10. "Magnetic and electrical properties of In doped cobalt ferrite nanoparticles | Journal of Applied Physics AIP Publishing." Accessed: Oct. 25, 2024. https://pubs.aip.org/aip/jap/article-
11. S. Dabas, M. Chahar, and O. P. Thakur, "Electromagnetic interference shielding properties of CoFe2O4/polyaniline/poly (vinylidene fluoride) nanocomposites," *Mater. Chem. Phys.*, vol. 278, p. 125579, Feb. 2022, doi: 10.1016/j.matchemphys.2021.125579.
12. B. Chethan, V. Prasad, S. Mathew, and H. Jan, "Polyaniline/Graphene oxide composite as an Ultra-Sensitive humidity sensor," *Inorg. Chem. Commun.*, vol. 166, p. 112633, Aug. 2024, doi: 10.1016/j.inoche.2024.112633.
13. M. Mishra, A. P. Singh, V. Gupta, A. Chandra, and S. K. Dhawan, "Tunable EMI shielding effectiveness using new exotic carbon: Polymer composites," *J. Alloys Compd.*, vol. 688, pp. 399–403, Dec. 2016, doi: 10.1016/j.jallcom.2016.07.190.
14. "(PDF) The Effect of a Small Amount of Water on the Structure and Electrochemical Properties of Solid-State Synthesized Polyaniline." Accessed: Oct.26,2024. https://www.researchgate.net/publication/258684418
15. E. Tanrıverdi, A. ÜZÜMCÜ, H. Kavas, A. Demir Korkmaz, and A. Baykal, "Conductivity Study of Polyaniline-Cobalt Ferrite (PANI-CoFe2O4) Nanocomposite," *Nano-Micro Lett.*, vol. 3, pp. 99–107, Jul. 2011, doi: 10.1007/BF03353658.
16. N. Maruthi *et al.*, "Polyaniline/V2O5 composites for anticorrosion and electromagnetic interference shielding," *Mater. Chem. Phys.*, vol. 259, p. 124059, Feb. 2021, doi: 10.1016/j.matchemphys.2020.124059.
17. M. A. Ahmed, R. M. Khafagy, S. T. Bishay, and N. M. Saleh, "Effective dye removal and water purification using the electric and magnetic Zn0.5Co0.5Al0.5Fe1.46La0.04O4/polymer core–shell nanocomposites," *J. Alloys Compd.*, vol. 578, pp. 121–131, Nov. 2013, doi: 10.1016/j.jallcom.2013.04.182.
18. C. Shekhar Joshi, R. C. Srivastava, and A. Joshi, "Polyaniline/Manganese-Cobalt ferrite nanocomposite as an efficient material for crystal violet dye degradation under sunlight irradiation," *Mater. Today, Proc.*, May 2023, doi: 10.1016/j.matpr.2023.04.462.
19. S. S. Menon, M. Thomas, and M. T. Ramesan, "Synthesis, characterization, gas sensing, and electrical property evaluation of polyaniline/copper-alumina nanocomposites," *Polym. Compos.*, vol. 41, no. 3, pp. 900–910, 2020, doi: 10.1002/pc.25421.
20. B. Ünal, "The Electrical Properties of Polyaniline (PANI)–Co0.5Mn0.5Fe2O4 Nanocomposite," *J. Inorg. Organomet. Polym. Mater.*, Jan. 2013, Accessed: Oct. 26, 2024. [Online]. Available: https://www.academia.edu/106413187/
21. S. Naseem, "Synthesis of Polyaniline/$^{\gamma}$-Fe 2 O 3 Nanocomposites and Study of their Structural and Electrical Properties", Accessed: Oct. 26, 2024. https://www.academia.edu/33417973/
22. "Nanoclay-based conductive and electromagnetic interference shielding properties of silver-decorated polyaniline and its nanocomposites - Materials Advances (RSC Publishing)." Accessed: Oct.25,2024. https://pubs.rsc.org/en/content/articlelanding/2023/ma/d3ma00393k
23. S. B. Aziz, A. Marf, E. Dannoun, M. Brza, and R. Abdullah, "The Study of the Degree of Crystallinity, Electrical Equivalent Circuit, and Dielectric Properties of Polyvinyl Alcohol (PVA)-Based Biopolymer Electrolytes," *Polymers*, vol. 12, Sep. 2020 doi: 10.3390/polym12102184.
24. "Interfacial Polarization-Induced Loss Mechanisms in Polypropylene/BaTiO3 Nanocomposite Dielectrics | Chemistry of Materials." Accessed: Oct. 25, 2024. https://pubs.acs.org/doi/abs/10.1021/acs.chemmater.6b01383
25. G. Harisha *et al.*, "Synthesis and characterization of PANI-CZF nanocomposites for enhanced electromagnetic interference shielding," *J. Mater. Sci. Mater. Electron.*, vol. 35, no. 6, p. 391, Feb. 2024, doi: 10.1007/s10854-024-12086-6.
26. A. Kausar and I. Ahmad, "Conducting Polymer Nanocomposites for Electromagnetic Interference Shielding—Radical Developments," *J. Compos. Sci.*, vol. 7, p. 240, Jun. 2023, doi: 10.3390/jcs7060240.
27. "Progressive Review of Functional Nanomaterials-Based Polymer Nanocomposites for Efficient EMI Shielding." Accessed: Oct. 26, 2024. https://www.mdpi.com/2504-477X/7/2/77
28. "(PDF) Electromagnetic Interference Impacts on Electronic Systems and Regulations." Accessed: Oct. 26, 2024. https://www.researchgate.net/publication/377181966
29. "Super flexible Interconnected Graphene Network Nanocomposites for High-Performance Electromagnetic Interference Shielding | ACS Omega." Accessed: Oct. 26, 2024. [Online]. Available: https://pubs.acs.org/doi/10.1021/acsomega.8b00432
30. "Polymer Nanocomposites for Electromagnetic Interference Shielding...: Ingenta Connect." Accessed: Oct. 26, 2024. https://www.ingentaconnect.com/content/asp/jnn/2018/00000018/00000011/art00055;jsessionid=w0dn349nrf3i.x-ic-live-03
31. "Chemically reduced versus photo-reduced clay-Ag-polypyrrole ternary nanocomposites: Comparing thermal, optical, electrical and

electromagnetic shielding properties | CoLab.” Accessed: Oct. 26, 2024. https://colab.ws/articles/10.1016%2Fj.materresbull.2016.05.024

32. “Preparation of silver-plated polyimide fabric initiated by polyaniline with electromagnetic shielding properties - Dan Yu, Yu Wang, Tianqi Hao, Wei Wang, Baojiang Liu, 2018.” Accessed: Oct. 26, 2024.: https://journals.sagepub.com/doi/full/10.1177/1528083717692592
33. S. Manjunatha, T. Machappa, Y. T. Ravikiran, B. Chethan, and A. Sunilkumar, “Polyaniline based stable humidity sensor operable at room temperature,” *Phys. B Condens. Matter*, vol. 561, pp. 170–178, May 2019, doi: 10.1016/j.physb.2019.02.063.
34. “Humidity sensing properties of poly-vanadium-titanium acid combined with polyaniline grown in situ by electrochemical polymerization - ScienceDirect.” Accessed: Oct. 25, 2024. [Online]. Available: https://www.sciencedirect.com/science/article/abs/pii/S0925400518309110?via%3Dihub
35. “Chemisorption and Physisorption of Water Vapors on the Surface of Lithium-Substituted Cobalt Ferrite Nanoparticles | ACS Omega.” Accessed: Oct25,2024. https://pubs.acs.org/doi/10.1021/acsomega.0c04784
36. “Full article: Humidity-sensing properties of conducting polypyrrole-silver nanocomposites.” Accessed: Oct. 25, 2024. https://www.tandfonline.com/doi/full/10.1080/17458080802512494
37. “Grotthuss mechanism.” Accessed: Oct. 25, 2024. https://water.lsbu.ac.uk/water/grotthuss.html#alt
38. L. Kabir, A. R. Mandal, and S. K. Mandal, “Humidity-sensing properties of conducting polypyrrole-silver nanocomposites,” *J. Exp. Nanosci.*, vol. 3, no. 4, pp. 297–305, Dec. 2008, doi: 10.1080/17458080802512494.

## AUTHORS:

**Raghavendra Naik** received his B Sc degree from Karnataka University Dharwad, India in 2021 and MSc degree in Organic Chemistry at Alva’s college Moodbidri, Karnataka, India in 2023. He is currently pursuing PhD at the Department of Chemistry, PES University Bangalore.
E-mail: raghavendranaik334@gmail.com

**Revanasiddappa M** received his BSc degree in from Vijayanagar college Hosapet affiliated to Gulbarga University Gulbarga in the year 1997. Completed masters in Inorganic chemistry in the year 1999, M.Phil., in 2000 and Ph.D., in 2006 from Gulbarga University, Gulbarga, working as Professor of Chemistry, P E S University Electronic city campus. His projects have been funded by VTU, TEQIP and VGST-K FIST (L1). Synthesized the Novel macrocyclic ligands of symmetric and asymmetric azines by using Benzophenone hydrazones and their coordination metal Complexes of first row transition metal ions. Prepared ligands and complexes were characterized by using techniques such as UV-Visible, IR, NMR, ESR, Magnetic Susceptibility Measurement and XRD. Detailed studies of their antimicrobial and electrical properties such as DC properties were investigated. His current research area is the ever-increasing application of conducting polymers, in various fields of science and technology is the driving force for selecting this topic, he has presented research articles in National/International conferences and published research papers in various International and Nations Journals; He has few honors and recognitions to his credits.
E-mail: revanasiddappam@pes.edu

**Manjunatha . S** received his M.Sc. in Physics from Gulbarga University, Kalaburagi, in 2008 and Post-Graduate Diploma in Materials Science in 2010 from Jawaharlal Nehru Centre for Advanced Scientific Research (JNCASR), Bengaluru. Later he worked as a R&D Asst. in Prof. C.N.R. Rao’s lab and Prof. S.M. Shivaprasad’s Lab at JNCASR. He obtained his Ph.D. in Physics in 2021 from Visvesvaraya Technological University, Belagavi. His research interests are conductivity and sensing studies of conducting polymer composites, functionalization of transition metal dichalcogenides.
E-mail: manjusballari@gmail.com

**Y.T Ravikiran** He received his M.Sc. degree in Physics in 2002 and M.Phil. degree in 2003, and Ph.D.
degree in Physics in 2008 from Gulbarga University, India. He is currently Assistant Professor of Physics in Government Science College, Chitradurga, India. He has published 89 articles in international pre-revived journals. His research interests are sensors, nanomaterials, polymers, magnetic materials, energy storage devices, solar cells etc.
E-mail: ytrcta@gmail.com